Electron–Phonon Interactions in Single Octanedithiol Molecular Junctions

Joshua Hihath, Christopher Bruot, and Nongjian Tao*

Center for Bioelectronics and Biosensors, the Biodesign Institute, and Department of Electrical Engineering, Arizona State University, Tempe, Arizona 85287-5801

ARTICLE

ABSTRACT We study the charge transport properties and electron–phonon interactions in single molecule junctions, each consisting of an octanedithiol molecule covalently bound to two electrodes. Conductance measurements over a wide temperature range establish tunneling as the dominant charge transport process. Inelastic electron tunneling spectroscopy performed on individual molecular junctions provides a chemical signature of the molecule and allows electron–phonon interaction induced changes in the conductance to be explored. By fitting the conductance changes in the molecular junction using a simple model for inelastic transport, it is possible to estimate the phonon damping rates in the molecule. Finally, changes in the inelastic spectra are examined in relation to conductance switching events in the junction to demonstrate how changes in the configuration of the molecule or contact geometry can affect the conductance of the molecular junction.

KEYWORDS: molecular electronics · molecular conductance · inelastic electron tunneling spectroscopy · IETS · break junction

Molecular electronics has made significant advances in recent years, and molecular systems exhibiting gate effects, rectification, and switching behavior have all been identified and studied.[1] With such impressive progress it is becoming increasingly important to understand the fundamental electron transport properties. Inelastic electron tunneling spectroscopy (IETS) has become an important tool for characterizing molecular junctions because it provides a direct chemical signature of the molecules in the junction, and can be compared with theory.[2−14] More importantly, IETS probes electron–phonon interactions, which are closely related to carrier dephasing and changes in the contact configuration in single molecule junctions, which are the focus of the present study. Using a low-temperature STM-break junction configuration, electron–phonon interactions in many individual junctions were measured to determine the reproducibility and variability of the phonon modes between junctions, and the dependence of the phonon modes on the detailed molecule–electrode contact geometry. Furthermore, by studying a single molecule that is covalently bound to two electrodes, the conductance changes due to individual phonon modes in the molecular junction were precisely measured, making it possible to estimate the phonon damping rates from the conductance changes.

The dominant transport mechanism in many molecular junctions is elastic tunneling, which means that the majority of power dissipated due to carrier transport occurs in the contacts. However, inelastic tunneling is also possible and requires that some energy is transferred from the carriers to the molecule. Huang *et al.*[15,16] have measured the local temperature of molecular junctions and found that the junction temperature increases at low biases due to electron–phonon interactions, and eventually decreases due to electron–electron interactions. In the present study we determine specific electron–phonon interactions in a single molecule junction, and how these modes affect the transport probability. To achieve this goal, we examine the conductance of single octanedithiol molecular junctions over a wide temperature range to demonstrate that tunneling is the dominate transport mechanism and perform IETS on individual junctions at 4.2 K to obtain a chemical signature for the junction, examine the phonon damping rates, probe the specific conductance changes in the molecules under an applied bias, and explore the effects of junction configuration on the conductance and IETS response of the junctions.

To establish the conductance of a single octanedithiol junction and establish the charge transport mechanism, we used an STM break junction technique,[17] where an STM tip is brought into contact with a

*Address correspondence to nongjian.tao@asu.edu.

Received for review March 8, 2010 and accepted June 09, 2010.

Published online June 16, 2010.
10.1021/nn100470s

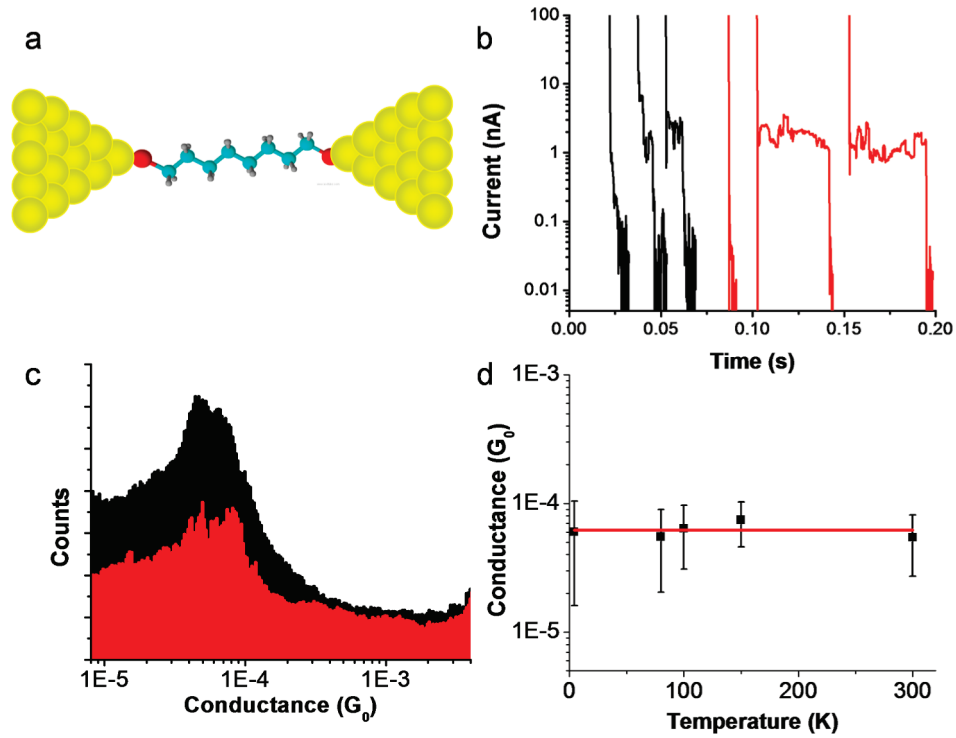

Figure 1. (a) A molecular junction consisting of a single octanedithiol molecule bound to two electrodes. (b) STM break-junction measurements taken at 300 K (black curves) and 4.2 K (red curves), both show clear steps, but at low temperature the features are much more distinct. (c) Two conductance histograms constructed from thousands of curves similar to those shown in panel b. The black histogram is for 300K and the red histogram is for 4.2K. (d) Peak values of conductance histograms taken at several temperatures between 4.2 and 300 K with a bias of 300 mV. The conductance is independent of temperature indicating tunneling behavior for the octanedithiol molecule.

monolayer of dithiol molecules capable of forming a Au−S bond between the electrodes and the molecule and then retracting the tip to observe steps in the current *versus* distance traces, which occur in the tunneling regime below the conductance quantum, $G_o = 2e^2/h$. These steps, as is shown in Figure 1, have been ascribed to the presence of molecules between the tip and the substrate, and a statistical analysis of thousands of these current *versus* distance traces yields peaks representing the most likely conductance of a single molecule junction.[18−23] Break-junction measurements were carried out in a home-built STM under high vacuum between 300 and 4 K, and the results demonstrate that the conductance does not change within this temperature regime. The average conductance in this regime was found to be $\sim 6.2 \times 10^{-5} G_o$, which agrees well with the other values found in literature.[19,20,24−26] Although these histograms show pronounced peaks, the features are quite broad, and it is not possible to discern differences between one and two molecules in the junction. However, if a linear bin is used for the statistical analysis, these features become more obvious, but then it is not possible to resolve the entire range.

Several of the tip retraction curves are shown in Figure 1b for both the room temperature and 4.2 K case. In each of these cases, there are obvious steps in the current around 1 nA; however, the steps that occur at 4.2 K are much longer than those at room temperature and show more distinct features in the plateau region. Furthermore, it was much more likely to observe steps in the retraction curves at room temperature than at 4.2 K, which is likely due to the increased stability and diminished drift at low temperature. Approximately 3000 curves were examined for constructing each of the histograms shown in Figure 1c, and the peak widths are quite similar despite the temperature change (the histograms have been offset for clarity). The temperature dependence of the conductance of single octanedithiol junctions have been previously measured in a narrow temperature range near room temperature with differing conclusions.[24,26] One experiment demonstrated temperature independent conductance,[24] and the other demonstrated that the conductance followed Arrhenius behavior.[26] These discrepancies are likely due to the two methods probing different molecular conformations. Furthermore, nanopore junctions with several thousand molecules present have been used for wide-range temperature dependence studies, and demonstrated temperature independent conductance.[4,27] However, it has not yet been possible to perform a statistical analysis of thousands of single molecule junctions over a wide temperature range to explore the temperature dependence of the conductance. The conductance *versus* temperature is plotted in Figure 1d, and shows that the conductance is independent of temperature over a range of ~300 K, clearly implicat-

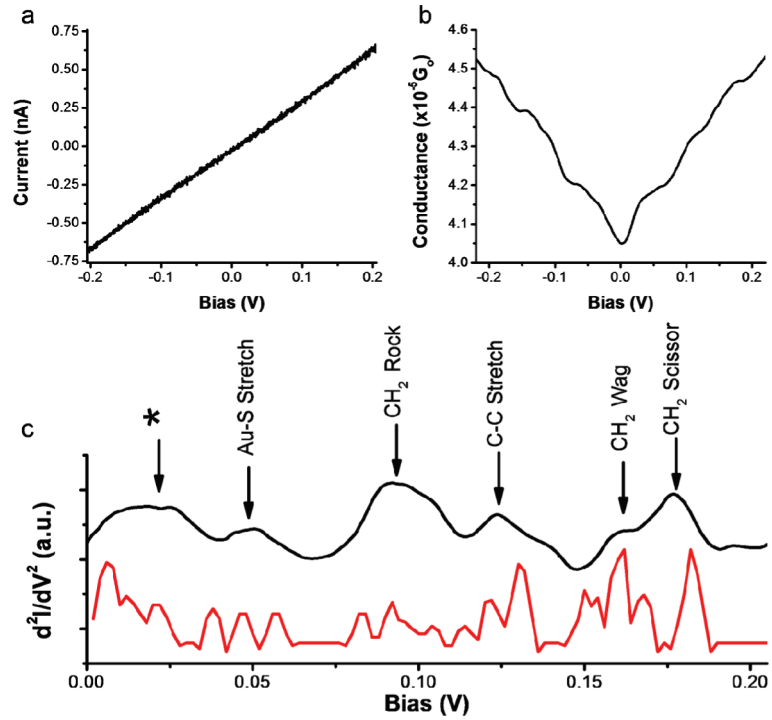

Figure 2. An example of IETS measurements and peak assignments: (a) averaged *I*−*V* curve from 18 different bias sweeps; (b) averaged conductance (*G*) *vs* bias from the same curves obtained with a lock-in amplifier; (c) IETS obtained by taking the numerical derivative from panel b (black curve), and phonon modes obtained from a DFT calculation of the molecular junction used for assigning peaks (red curve).

ing tunneling as the conductance mechanism for octanedithiol single molecule junctions.

Once the conductance was determined and the transport mechanism was established, it was possible to proceed with IETS measurements. In a tunneling junction with only elastic scattering present, one would expect the *I*−*V* curve to be linear in the low bias regime where the energy levels are far from resonance. However, when inelastic tunneling pathways associated with the excitation of phonon modes are opened in the tunneling junction, nonlinearities occur in the *I*−*V* curve. At low temperatures, the probability of the phonon modes being excited thermally is extremely low. But, when the applied bias voltage exceeds $V_\omega = \hbar\omega/e$, where ω is the frequency of a phonon mode, $\hbar$ is the Planck constant, and *e* is the electron charge, the phonon mode with energy $\hbar\omega$ can be excited *via* electron−phonon interactions.[28,29] This excitation of the phonon modes leads to an additional tunneling pathway and an increase in the conductance (for molecular junctions with conductance less than $0.5G_o$).[30]

Although additional pathways create nonlinearities in the *I*−*V* curve, it is often difficult to extract specific information about the energy of the modes and the relative change in the conductance. Because of this difficulty, it is more common to measure d*I*/d*V* *versus* *V* (*G*−*V*) where the excitation of an inelastic mode can be seen as a step, or to measure d^2*I*/d*V*^{2} *versus* *V*, referred to as the IET spectrum, where the excitation energy for the phonon mode appears as a peak or a dip. These junctions are symmetric, and the excitation of these modes depends only on the magnitude of the bias applied across the junction and not on the polarity. Therefore, steps in the *G*−*V* traces due to the excitation of phonon modes should be symmetric about zero bias, and the peaks in the IET spectra should exhibit antisymmetric behavior, that is, $d^2I(V)/dV^2 = -d^2I(-V)/dV^2$.[31] As there are a myriad of other processes which can cause peaks in the IET spectrum, such as interference or impurity scattering in the leads,[32] only peaks with clearly antisymmetric behavior in the IET spectra will be identified as phonon modes in the following discussion.

To perform IETS measurements on a single molecule junction one must first be certain that a molecule is attached covalently to both electrodes. To achieve this certainty, measurements were performed in a manner similar to the conductance experiments described above. First, the STM tip is brought into contact with the surface and then retracted. If a molecule bridges the two electrodes, a step occurs in the current *versus* distance trace, but in this case rather than continuing to retract the tip until the junction breaks down, the withdraw process is stopped so that the bias can be swept to record the *I*−*V*, *G*−*V*, and IET spectra. Figure 2 shows an example of *I*−*V*, *G*−*V*, and IETS curves obtained by averaging 18 curves collected from several independent junctions. The *I*−*V* curve is not simply linear, but it is difficult to extract specific information from this curve. Figure 2b plots the *G*−*V* trace,

which shows more clearly the nonlinearity and features due to phonon modes in the I−*V* curve. The conductance, as shown in Figure 2b, is 4.05 × $10^{-5}G_o$ near zero bias, but it increases to 4.5 × $10^{-5}G_o$ at 200 mV. This corresponds to an increase in the conductance of over 10%, which indicates a substantial contribution of phonon modes in the conductance as the bias increases. Note also that this conductance value and percent change is also consistent with the histograms shown in Figure 1c, which were obtained at 300 mV.

Figure 2c shows the IET spectrum obtained by taking the numerical derivative of the *G*−*V* curve in Figure 2b (black curve). We focus here on the spectrum in the region below 200 mV as all modes except those for the C−H stretch are expected to be in this region. To make assignments of the peak positions, comparisons were made with a vibrational spectrum obtained from a DFT calculation using Gaussian 03W[33] and the b3lyp/lanl2dz basis set for the octanedithiol molecular junction with 1 gold atom attached to each sulfur (red curve, Figure 2c), and a reported scaling factor of 0.97.[34] The red curve was obtained, by counting the number of vibrational modes in each 2 mV interval, thus creating an effective density of phonon states. Since related vibrational modes are often clustered in energy, this provided a straightforward method of assigning peak positions. These assignments also correlate well with theoretical and experimental studies of related systems.[9,10,35−39] The peak near 17 mV, marked with an asterisk (*), was not assigned because there are a variety of modes that may occur near this energy, such as a Au−Au stretch,[40] a C−C−C scissor,[9] or a $(CH_2)_2$ twist;[10] this can also be seen from the density of phonon modes in this region. The mode at 48 mV is likely due to a Au−S stretch, but it should be noted that the DFT calculation shows that this mode also includes a significant scissoring motion of the carbon backbone, and as such this assignment is consistent with previous assignments near this energy.[9,39]

IETS has previously been performed on octanedithiol junctions in self-assembled monolayer junctions,[4,36] and in electromigrated junctions.[37] Although the experiments presented here are significantly different in that it is possible to measure a large number of single molecular junctions and explore how energies and intensities can change between junctions (as is discussed in detail below), these results still possess similarities and differences with each of these studies. The resolution of several peaks below 100 mV was only reported by one group;[4] however, that result also showed significant peaks and dips in the IET spectra, which are not apparent in this study. Several of the peaks are similar to those found in either electromigrated junctions or in cross-wire systems.[36,37] The most significant difference between these studies is in the peak at 80 mV due to a C−S stretch which is clear in both of the previous studies, but is only visible in a few of the junctions measured, and is not apparent in the averaged spectra presented here.

Assigning peaks using IETS provides a chemical signature for the junction, but it is of more interest to discern how each of these modes affects the total conductance of the molecular junction. A full treatment of electron transport in molecules involving electron−phonon interactions often requires significant computational effort. However, theoretical treatments of inelastic tunneling were derived decades ago,[41] and recently similar, computationally inexpensive approaches have been used to describe experimental data using only the transmission function, τ, the electron−hole and external damping rates, γ_{eh} and γ_d, and the phonon frequency, ω, as fitting parameters.[30,42] The assumptions for using this simplified model are that (i) the electron−phonon coupling is weak and (ii) the density of states of the contacts and the device are slowly varying near the Fermi energy of the electrodes. The second assumption seems well justified since the transmission probability indicates the system is far from resonance. The first assumption implies that multiphonon processes are rare, and that the phonon modes have little effect on the elastic component of the transmission probability, although this seems like a reasonable assumption for this type of molecular system, it may not always be the case, and will be discussed in greater detail below. We apply this model by including the first three phonon modes and obtain[30,41]

$$I = \frac{e^2}{\pi\hbar^2}\tau V + \frac{1-2\tau}{4}\pi\sum_{\lambda} I_{sym}\frac{\gamma_{eh\lambda}}{\omega_\lambda} \quad (1)$$

$$I_{sym} = \frac{e}{\pi\hbar}\left(2eVn_\lambda + \frac{\hbar\omega_\lambda - eV}{\exp\left(\frac{\hbar\omega_\lambda - eV}{kT}\right) - 1} - \frac{\hbar\omega_\lambda + eV}{\exp\left(\frac{\hbar\omega_\lambda - eV}{kT}\right) - 1}\right) \quad (2)$$

where the first term in eq 1 is the same as the Landauer expression for the transport, and the second term is the contribution due to inelastic phonon scattering. In these equations n_λ is the bias dependent phonon occupation number including nonequilibrium heating,[6,43] *k* is the Boltzmann constant, and *T* is temperature. n_λ is determined by solving the steady-state rate equation for each phonon mode.[42] Although the application of these equations to a single phonon mode is straightforward, summing directly over the phonon modes neglects changes in the occupation due to the presence of additional phonons. Nevertheless, it provides an insightful estimation of the damping rates in the molecular junction and allows for a direct comparison between molecular species. Furthermore, it is also possible to estimate the total power dissipated in the molecule by using these fitting parameters, and this application

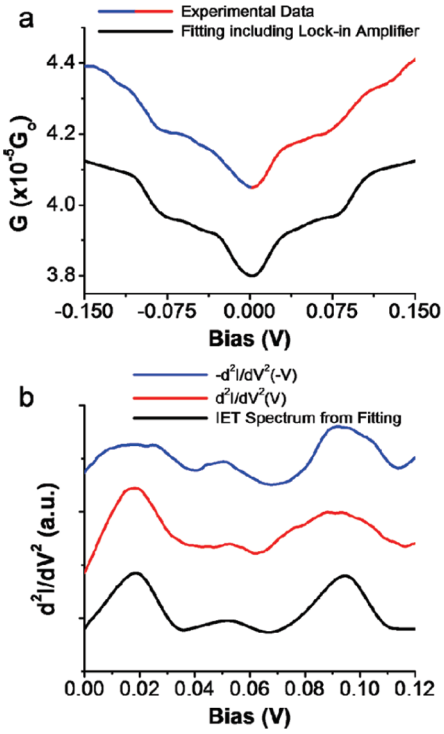

Figure 3. Fitting of IET spectrum of a single molecule junction. (a) Conductance (*G*) *versus* bias (*V*) curve averaged from 18 individual traces (red and blue curve) and fitted *G vs V* trace using the model in ref 30 (black curve), and including the effects of the AC modulation and low-pass filters from the lock-in amplifier. The data were offset for clarity. (b) IET spectra obtained from the part a. The red curve is the direct IET spectra, and the blue curve is $-d^2I(-V)/dV^2$, which is plotted to demonstrate the symmetry of the phonon modes with bias. The black curve is the derivative of the fitted *G*−*V* curve in part a.

of the model is discussed in the Supporting Information.

Figure 3a reproduces the *G*−*V* curve from Figure 2b in the ±150 mV range (red curve). The black curve is the result of fitting of the first three phonon modes using eq 1 above, and the graphs have been offset for clarity. In this fitting $\tau = 4.05 \times 10^{-5}$, the zero bias conductance extracted by fitting the small bias regime in the *I*−*V* curve, $\hbar\omega/e$ = 17, 48, and 93 mV, $\gamma_{eh} = 3.6 \times 10^7$, 2.5×10^7, and 1.4×10^8 s^{-1}, and $\gamma_d = 15\gamma_{eh}$, $5\gamma_{eh}$, and $1\gamma_{eh}$ for each of the three modes, respectively. The temperature was set to the experimental temperature of 4.2 K for each of these modes. Finally, the experimental technique was accounted for by including the AC modulation of 5 mV_{rms} along with the low-pass filter (3 Hz) of the lock-in amplifier to properly account for the experimental line-widths. Including these experimental parameters is extremely important to obtain a proper fitting because the majority of the line width broadening in these experiments is due to the experimental method rather than inherent to the molecular junction or the local temperature. The fitting with and without including the experimental broadening is included in the Supporting Information. Taking the derivative of the black curve in Figure 3a clearly shows the similarity of the fitted IET spectrum in both position and relative peak amplitude to that of the experimental junction plotted in Figure 3b (red and blue curves are experimental data and black curve is the derivative of the fitted curve). The modes are the same as described above and shown in Figure 2c.

Using this fitted model it is straightforward to extract the conductance change due to each phonon mode, and the conductance change for each of these conductance steps is 2.9%, 1.0%, and 3.1%, meaning that the addition of phonon modes significantly alters the total transmission function of a single molecule junction. Interestingly, these changes in the conductance are similar to those found in other alkanedithiol single molecule experiments, such as propanedithiol[7] and pentanedithiol.[39] Between these three systems the transmission probability changes by over 2 orders of magnitude, and in each of the three cases the tunneling transversal time is expected to be significantly different. However, the percent change in the conductance due to the excitation of phonon modes is similar in each of the cases. This finding suggests that the ratio γ_{eh}/τ is similar in all three cases despite the differences in length and the conductance of the molecules.

Thus far in the analysis we have assumed that the probability of multiphonon processes is relatively small. However, this may not always be a valid assumption even for a simple octanedithiol junction. As is discussed in detail in the theoretical literature, when the bias reaches sufficient energy to excite the phonon mode it is also possible for a carrier to both emit and absorb a phonon during transport.[30,44] This additional pathway can interfere with the primary elastic transport pathway and create a decrease in the conductance at the phonon energy even if the total conductance is much less than $0.5G_o$. Figure 4 shows one example where this may be the case.

Figure 4b is an average of 10 *G*−*V* curves obtained from the junction shown in Figure 4a. The *G*−*V* curve is symmetric below 150 mV, and the most obvious features in this regime are the local conductance minima near ±120 mV. The corresponding IET spectrum is shown in Figure 4c (red curve) along with the IET spectrum that was shown in Figure 3b (gray curve) for comparison. Although the peak intensities are considerably different for the two spectra, the first two peaks occur at similar energies while the third feature appears as a dip in the red curve and a peak in the gray curve. While there are a few possible explanations for such a feature in the IET spectrum, which cannot be ruled out, the symmetry of this feature in the *G*−*V* plot indicates that the effect is energy dependent, and the similarity in the energy of the dip feature in this IET spectrum to peaks in the IET spectrum of the other junctions presented suggests that it is due to a phonon mode. The differences in peak shape at this energy in the IET spectra demonstrate that the specific configuration of a

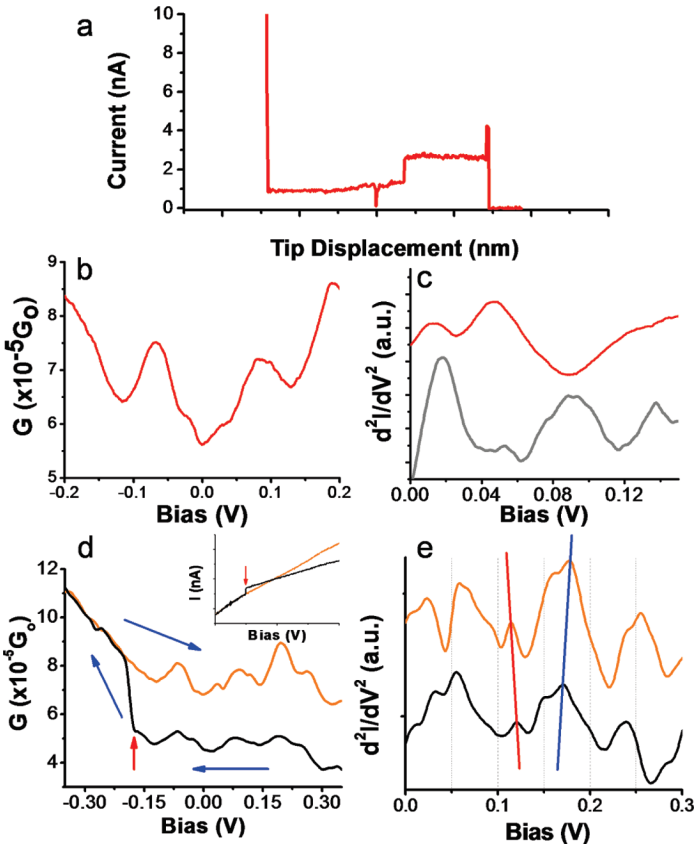

Figure 4. Phonon features in individual junctions. (a) Current *vs* distance trace for the junction shown in parts b−e. The bias was swept at various locations along the plateau region. (b) Average of 10 *G*−*V* curves from the junction shown in part a. There are clear decreases in the conductance of this junction with minima at ~|120 mV|. (c) The red curve is the IET spectrum obtained from part b. The gray curve is the same IET spectrum examined in Figure 3b. The locations of features in these two curves are similar, but the peak in the gray curve at 93 mV is seen as a dip in the red curve. (d) Two consecutive bias sweeps from the junction in part a. The features of the *G*−*V* curve are reproducible, but there is a clear switch in the conductance during the first sweep (black curve). The blue arrows indicate the direction of the bias sweeps, and the red arrow indicates the switching event. The inset shows the *I*−*V* curve. (e) The IET spectra from the two curves in part d. Although the general features of the two curves are similar, there are clear differences in the energies of certain peaks which can be either blue- or red-shifted after the conductance change as is indicated by the red and blue lines.

junction—either the contact geometry or the molecular configuration—can drastically influence the effects that phonon activation has on the molecular conductance.

In conjunction with these decreases in the conductance at defined energies, several other interesting features can be observed in individual *G*−*V* traces. Figure 4d shows two consecutive *G*−*V* traces obtained from the junction in Figure 4a, but which were not included in the average of Figure 4b. The most striking feature between these two curves is the switch in the conductance from a lower state to a higher state. The switch is quite clear in the *G*−*V* curve which is inset in Figure 4d. This behavior appears to be the switching of a single molecule junction into a higher conductance state rather than the attachment of a second molecule within the junction. The primary reason for this conclusion is that the features in both of the *G*−*V* curves (Figure 4d) and IET spectra (Figure 4e) are very similar. If a second molecule had bound between the tip and the substrate it is unlikely that the two molecules would have exactly the same configuration, and the *G*−*V* trace should have become an average of the signature of each of the molecules. A second reason is that shortly after the return sweep the junction broke and the conductance dropped to zero; again it is unlikely that two molecular junctions would break simultaneously.

Upon closer inspection of the IET spectrum for these curves, it is apparent that although the general features are similar there are significant variations in the absolute positions of the peaks in the two curves. It has been previously demonstrated that changes in the conductance of a single molecule junction can shift the energy of a peak in the spectrum to higher energies, and significantly alter the shape of the IET spectrum.[7] However, in this case the general features of the spectrum remain the same, and while the peak at ~170 mV is shifted to a higher energy, the peak at ~120 mV has shifted to a lower energy implying a small reorganization of the entire junction structure. These changes in the spectrum demonstrate how sensitive the conductance value is to small changes in the junction configuration. In this case, although the general features of the junction remain constant, small shifts in the locations of certain modes, indicating a change in the junction configuration, can change the conductance of the junction by approximately a factor of 2.

In summary we have performed STM break-junction experiments to determine the conductance properties of octanedithiol molecular junctions over a temperature range from 4.2 to 300 K, and the temperature independence of the conductance suggests tunneling behavior as is expected for this molecule. Once the conductance and transport mechanism was known, IETS measurements were performed on individual junctions to obtain a chemical signature of the molecular junction, to elucidate the electron−hole damping rates, and to determine the effects of electron−phonon interactions on molecular conductance. We also explored certain cases where decreases in the conductance were observed in single molecule junctions. These observations demonstrate that electron−phonon coupling can contribute significantly to the total conductance of a molecular junction, and that the specific configuration of the molecular junction can affect how a phonon mode changes the conductance. Finally, we observed a case where conductance switching occurred in a single molecule junction, in this case the change in conductance was approximately a factor of 2, and although the general features of the spectrum were the same before and after switching, the specific energies at which features occurred could shift to either higher or lower energy.

EXPERIMENTAL DETAILS

Sample Preparation. Octanedithiol samples were prepared by immersing a gold substrate in a ~1 mM solution of octanedithiol in toluene for 3−4 h. The gold substrates were prepared by thermal evaporation of 130 nm of gold (99.9999% purity, Alfa Aesar) on a freshly cleaved mica surface (Ted Pella, Inc.). Prior to immersion in the octanedithiol solution the substrate was annealed in a hydrogen flame for approximately 1 min. Once the substrate was removed from the solution it was promptly placed in the homemade STM head along with a newly cut gold tip (99.998% purity Alfa Aesar). The system was then placed in a helium Dewar cryostat (Janis Research Company). The STM chamber was place under a vacuum of 2×10^{-6} Torr before any cryogens were introduced to the system. Once the system stabilized in temperature to ~4.2 K, break junction and IETS measurements were performed. Break-junction measurements at higher temperatures were collected by heating the STM head *via* a resistive heater in the sample chamber, and room temperature measurements were performed in vacuum prior to cooling the STM.

Break-Junction and IETS Measurements. Break-junction measurements were performed using LabView software and a National Instruments data acquisition card (PCIe-6289) for controlling the high-voltage piezo and bias drivers which were designed and built in-house, as well as for monitoring the current. The break-junction measurements were performed using the tip−substrate current as the feedback signal, and driving the tip into the substrate until the current amplifier (10 nA/V) saturated, after which the tip was withdrawn and the resulting current *versus* distance trace was recorded. Approximately 3000 cycles were recorded for each bias and temperature prior to constructing the histograms. Each histogram was constructed by binning the current *versus* distance traces on a logarithmic scale, and adding curves to the histogram using an automated algorithm that rejected curves that exhibited spikes in the current or long decay times. Each of the histograms is constructed from ~60% of the collected data for a specific bias.

IETS measurements were performed in a similar method as the break-junction measurements, except that the program was set to stop automatically if a plateau occurred in the current *versus* distance trace. Once the tip withdraw was stopped, the bias was swept over a ±400 mV range. The current was then recorded directly from the current amplifier, and the $G-V$ curves were obtained using a standard lock-in amplifier technique.[45] A 4.33 kHz AC signal of 5 mV_{rms} was added to the bias for the lock-in amplifier (5110 Princeton Applied Research). The IET spectra were obtained by taking the numerical derivative of the $G-V$ curves and smoothing the data using a Savitzky−Golay filter.

Acknowledgment. We are indebted to Nicolás Agraït for providing us with a low temperature STM scanner, Magnus Paulsson and Yoshihiro Asai for fruitful discussions, and the NSF(ECCS0925498) and DOE (DE-FG02-01ER45943) for financial support.

Supporting Information Available: A description of the model used for fitting the experimental data, as well as a discussion of the power dissipation. This material is available free of charge *via* the Internet at http://pubs.acs.org.

REFERENCES AND NOTES

1. Tao, N. J. Electron Transport in Molecular Junctions. *Nat. Nanotechnol.* **2006**, *1*, 173–181.
2. Park, H.; Park, J.; Lim, A. K. L.; Anderson, E. H.; Alivisatos, A. P.; McEuen, P. L. Nanomechanical Oscillations in a Single-C60 Transistor. *Nature* **2000**, *407*, 58–60.
3. Stipe, B. C.; Rezaei, M. A.; Ho, W. Single-Molecule Vibrational Spectroscopy and Microscopy. *Science* **1998**, *280*, 1732–1735.
4. Wang, W.; Lee, T.; Kretzschmar, I.; Reed, M. A. Inelastic Electron Tunneling Spectroscopy of an Alkanedithiol Self-Assembled Monolayer. *Nano Lett.* **2004**, *4*, 643–646.
5. Kushmerick, J. G.; Lazorcik, J.; Patterson, C. H.; Shashidhar, R.; Seferos, D. S.; Bazan, G. C. Vibronic Contributions to Charge Transport across Molecular Junctions. *Nano Lett.* **2004**, *4*, 639–642.
6. Paulsson, M.; Frederiksen, T.; Brandbyge, M. Inelastic Transport through Molecules: Comparing First-Principles Calculations to Experiments. *Nano Lett.* **2006**, *6*, 258–262.
7. Hihath, J.; Arroyo, C. R.; Rubio-Bollinger, G.; Tao, N.; Agrait, N. Study of Electron−Phonon Interactions in a Single Molecule Covalently Connected to Two Electrodes. *Nano Lett.* **2008**, *8*, 1673–1678.
8. Djukic, D.; Thygesen, K. S.; Untiedt, C.; Smit, R. H. M.; Jacobsen, K. W.; van Ruitenbeek, J. M. Stretching Dependence of the Vibration Modes of a Single-Molecule Pt−H_2−Pt Bridge. *Phys. Rev. B: Condens. Matter* **2005**, *71*, 161402/1–161402/4.
9. Solomon, G. C.; Gagliardi, A.; Pecchia, A.; Frauenheim, T.; Di Carlo, A.; Reimers, J. R.; Hush, N. S. Understanding the Inelastic Electron-Tunneling Spectra of Alkanedithiols on Gold. *J. Chem. Phys.* **2006**, *124*, 094704/1–094704/10.
10. Pecchia, A.; Di Carlo, A. Incoherent Electron-Phonon Scattering in Octanethiols. *Nano Lett.* **2004**, *4*, 2109–2114.
11. Chen, Y.-C.; Zwolak, M.; Di Ventra, M. Inelastic Effects on the Transport Properties of Alkanethiols. *Nano Lett.* **2005**, *5*, 621–624.
12. Osorio, E. A.; O'Neill, K.; Stuhr-Hansen, N.; Nielsen, O. F.; Bjornholm, T.; van der Zant, H. S. J. Addition Energies and Vibrational Fine Structure Measured in Electromigrated Single-Molecule Junctions Based on an Oligophenylenevinylene Derivative. *Adv. Mater. (Weinheim, Ger.)* **2007**, *19*, 281–285.
13. Troisi, A.; Ratner, M. A. Molecular Transport Junctions: Propensity Rules for Inelastic Electron Tunneling Spectra. *Nano Lett.* **2006**, *6*, 1784–1788.
14. Asai, Y. Nonequilibrium Phonon Effects on Transport Properties through Atomic and Molecular Bridge Junctions. *Phys. Rev. B: Condens. Matter* **2008**, *78*, 0454341/045434−24.
15. Huang, Z.; Chen, F.; D'Agosta, R.; Bennett, P. A.; Di Ventra, M.; Tao, N. Local Ionic and Electron Heating in Single-Molecule Junctions. *Nat. Nanotechnol.* **2007**, *2*, 698–703.
16. Huang, Z. F.; Xu, B. Q.; Chen, Y. C.; Di Ventra, M.; Tao, N. J. Measurement of Current-Induced Local Heating in a Single Molecule Junction. *Nano Lett.* **2006**, *6*, 1240–1244.
17. Xu, B.; Tao, N. J. Measurement of Single-Molecule Resistance by Repeated Formation of Molecular Junctions. *Science* **2003**, *301*, 1221–1223.
18. Ulrich, J.; Esrail, D.; Pontius, W.; Venkataraman, L.; Millar, D.; Doerrer, L. H. Variability of Conductance in Molecular Junctions. *J. Phys. Chem. B* **2006**, *110*, 2462–2466.
19. Gonzalez, M. T.; Wu, S.; Huber, R.; van der Molen Sense, J.; Schonenberger, C.; Calame, M. Electrical Conductance of Molecular Junctions by a Robust Statistical Analysis. *Nano Lett.* **2006**, *6*, 2238–42.
20. Li, C.; Pobelov, I.; Wandlowski, T.; Bagrets, A.; Arnold, A.; Evers, F. Charge Transport in Single Au|Alkanedithiol|Au Junctions: Coordination Geometries and Conformational Degrees of Freedom. *J. Am. Chem. Soc.* **2008**, *130*, 318–326.
21. Smit, R. H. M.; Noat, Y.; Untiedt, C.; Lang, N. D.; van Hemert, M. C.; van Ruitenbeek, J. M. Measurement of the Conductance of a Hydrogen Molecule. *Nature* **2002**, *419*, 906–909.
22. Lortscher, E.; Weber, H. B.; Riel, H. Statistical Approach to Investigating Transport through Single Molecules. *Phys. Rev. Lett.* **2007**, *98*, 176807/1–176807/4.
23. Taniguchi, M.; Tsutsui, M.; Yokota, K.; Kawai, T. Inelastic Electron Tunneling Spectroscopy of Single-Molecule Junctions Using a Mechanically Controllable Break Junction. *Nanotechnology* **2009**, *20*, 434008/1–434008/8.
24. Li, X.; He, J.; Hihath, J.; Xu, B.; Lindsay, S. M.; Tao, N. Conductance of Single Alkanedithiols. Conduction Mechanism and Effect of Molecule-Electrode Contacts. *J. Am. Chem. Soc.* **2006**, *128*, 2135–2141.
25. Jang, S.-Y.; Reddy, P.; Majumdar, A.; Segalman, R. A.

Interpretation of Stochastic Events in Single Molecule Conductance Measurements. *Nano Lett.* **2006**, *6*, 2362–2367.
26. Haiss, W.; van Zalinge, H.; Bethell, D.; Ulstrup, J.; Schiffrin, D. J.; Nichols, R. J. Thermal Gating of the Single Molecule Conductance of Alkanedithiols. *Faraday Discuss.* **2006**, *131*, 253–264.
27. Wang, W. Y.; Lee, T. H.; Reed, M. A. Electronic Transport in Molecular Self-Assembled Monolayer Devices. *Proc. IEEE* **2005**, *93*, 1815–1824.
28. Lambe, J.; Jaklevic, R. C. Molecular Vibration Spectra by Inelastic Electron Tunneling. *Phys. Rev.* **1968**, *165*, 821–32.
29. Jaklevic, R. C.; Lambe, J. Molecular Vibration Spectra by Electron Tunneling. *Phys. Rev. Lett.* **1966**, *17*, 1139–40.
30. Paulsson, M.; Frederiksen, T.; Brandbyge, M. Modeling Inelastic Phonon Scattering in Atomic- and Molecular-Wire Junctions. *Phys. Rev. B: Condens. Matter* **2005**, *72*, 2011011/201101−4.
31. Walczak, K. Vibrational Features in Inelastic Electron Tunneling Spectra. *Chem. Phys.* **2007**, *333*, 63–68.
32. Agrait, N.; Yeyati, A. L.; van Ruitenbeek, J. M. Quantum Properties of Atomic-Sized Conductors. *Phys. Rep.* **2003**, *377*, 81–279.
33. Frisch, M. J.; Trucks, G. W.; Schlegel, H. B.; Scuseria, G. E.; Robb, M. A.; Cheeseman, J. R.; Jr., J. A. M.; Vreven, T.; Kudin, K. N.; Burant, J. C., ; *et al*. *Gaussian 03, revision B.04*; Gaussian Inc.: Pittsburg, PA, 2003.
34. Pagliai, M.; Bellucci, L.; Muniz-Miranda, M.; Cardini, G.; Schettino, V. A Combined Raman, DFT and MD Study of the Solvation Dynamics and the Adsorption Process of Pyridine in Silver Hydrosols. *Phys. Chem. Chem. Phys.* **2006**, *8*, 171–178.
35. Wang, W.; Lee, T.; Reed, M. A. Elastic and Inelastic Electron Tunneling in Alkane Self-Assembled Monolayers. *J. Phys. Chem. B* **2004**, *108*, 18398–18407.
36. Yu, L. H.; Zangmeister, C. D.; Kushmerick, J. G. Structural Contributions to Charge Transport across Ni-Octanedithiol Multilayer Junctions. *Nano Lett.* **2006**, *6*, 2515–2519.
37. Song, H.; Kim, Y.; Jang, Y. H.; Jeong, H.; Reed, M. A.; Lee, T. Observation of Molecular Orbital Gating. *Nature* **2009**, *462*, 1039–1043.
38. Okabayashi, N.; Komeda, T. Inelastic Electron Tunneling Spectroscopy with a Dilution Refrigerator Based Scanning Tunneling Microscope. *Meas. Sci. Technol.* **2009**, *20*, 095602-1–095602-8.
39. Arroyo, C. R.; Frederiksen, T.; Rubio-Bollinger, G.; Vélez, M.; Arnau, A.; Sánchez-Portal, D.; Agraït, N. Characterization of Single-Molecule Pentanedithiol Junctions by Inelastic Electron Tunneling Spectroscopy and First-Principles Calculations. *Phys. Rev. B: Condens. Matter* **2010**, *81*, 075405-1–075405-5.
40. Agrait, N.; Untiedt, C.; Rubio-Bollinger, G.; Vieira, S. Onset of Energy Dissipation in Ballistic Atomic Wires. *Phys. Rev. Lett.* **2002**, *88*, 216803-1–216803-4.
41. Caroli, C.; Saintjam, D; Combesco, R; Nozieres, P. Direct Calculation of Tunnelling Current. 4. Electron−Phonon Interaction Effects. *J. Phys. C: Solid State Phys.* **1972**, *5*, 21–42.
42. Frederiksen, T.; Paulsson, M.; Brandbyge, M.; Jauho, A. P. Inelastic Transport Theory from First Principles: Methodology and Application to Nanoscale Devices. *Phys. Rev. B: Condens. Matter* **2007**, *75*, 205413.
43. Tikhodeev, S. G.; Ueba, H. Relation between Inelastic Electron Tunneling and Vibrational Excitation of Single Adsorbates on Metal Surfaces. *Phys. Rev. B: Condens. Matter* **2004**, *70*, 125414.
44. Galperin, M.; Ratner, M. A.; Nitzan, A. Inelastic Electron Tunneling Spectroscopy in Molecular Junctions: Peaks and Dips. *J. Chem. Phys.* **2004**, *121*, 11965–11979.
45. Petit, C.; Salace, G. Inelastic Electron Tunneling Spectrometer to Characterize Metal-Oxide-Semiconductor Devices with Ultrathin Oxides. *Rev. Sci. Instrum.* **2003**, *74*, 4462–4467.